COMPRESSION RESPONSE OF CRACKED REINFORCED CONCRETE

By F. J. Vecchio[1] and M. P. Collins,[2] Members, ASCE

ABSTRACT: Cracked reinforced concrete in compression has been observed to exhibit lower strength and stiffness than uniaxially compressed concrete. The so-called compression softening effect responsible is thought to be related to the degree of transverse cracking and straining present. It significantly influences the strength, ductility and load-deformation response of a concrete element. A number of experimental investigations have been undertaken to determine the degree of softening that occurs, and the factors that influence it. At the same time, a number of diverse analytical models have been proposed by various researchers aimed at modeling this behavior. In this paper, a review is made of the experimental data available, of the various models proposed, and of the accuracy of the models in correlating to the test data. Based on new data, previously derived analytical models are updated. Parametric studies are made to investigate factors thought to influence the softening effect. As well, nonlinear finite element analyses of test panels are conducted to determine the relative significance of compression softening in accurately predicting behavior of reinforced-concrete elements.

INTRODUCTION

The compression field theory (CFT) was originally formulated to model the behavior of reinforced-concrete beams subjected to torsion (Collins and Mitchell 1980). The theory treated cracked reinforced concrete in terms of average stresses and average strains, with the directions of principal stress and principal strain coinciding, and with the crack directions rotating. For cracked concrete in the principal compressive strain direction, the stress-strain response curve for plain concrete was adopted. No tensile stresses were assumed to exist in the concrete, in the principal tensile direction, after cracking.

In applying the CFT to model the results of various test specimens, it soon became evident that the response of cracked reinforced concrete in compression was substantially different from that of plain uniaxially compressed concrete (e.g., a concrete cylinder). The presence of large transverse tensile strains resulted in substantial reductions in the strength and stiffness of the concrete in compression (see Fig. 1). Hence, an experimental and theoretical investigation was undertaken to address this apparent compression softening effect. The resulting analytical model, known as the modified compression field theory (MCFT) (Vecchio and Collins 1986), introduced the following refinements: (1) A constitutive model for concrete in compression, reflecting the compression softening effects; (2) a constitutive model for cracked concrete in tension, reflecting the tension stiffening effects; and (3) checks of local stress conditions at crack locations.

The constitutive relations of the MCFT were subsequently incorporated into a number of nonlinear finite element programs [e.g., Stevens et al. (1991), Cook and Mitchell (1988), and Vecchio (1989)]. These programs

[1]Prof., Dept. of Civ. Engrg., Univ. of Toronto, Toronto, Canada M5S 1A4.
[2]Prof., Dept. of Civ. Engrg., Univ. of Toronto, Toronto, Canada M5S 1A4.

Note. Discussion open until May 1, 1994. To extend the closing date one month, a written request must be filed with the ASCE Manager of Journals. The manuscript for this paper was submitted for review and possible publication on June 8, 1992. This paper is part of the ***Journal of Structural Engineering***, Vol. 119, No. 12, December, 1993. ©ASCE, ISSN 0733-9445/93/0012-3590/$1.00 + $.15 per page. Paper No. 4184.

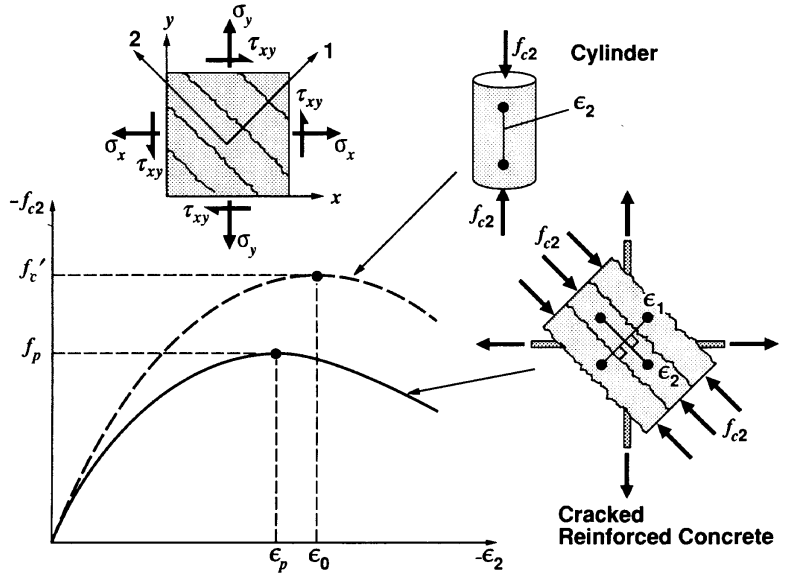

FIG. 1. Deteriorated Compression Response in Cracked Reinforced Concrete Elements

have been shown to accurately model behavior over a broad range of structural concrete elements and loading conditions. It is now generally agreed that some degree of compressive strength reduction is essential to accurately modeling behavior in cracked reinforced-concrete structures.

In the decade since the introduction of the MCFT compression softening model, considerably more work has been completed in investigating the phenomenon. A number of researchers have conducted independent test programs and have formulated alternative models. Naturally, there is some disagreement as to the degree of softening that occurs, and as to what factors influence it.

At the University of Toronto, a large number of tests have been completed since the original experimental investigation. The range of structural parameters and loading conditions encompassed is now larger. This expanded database presents the opportunity to reexamine the original MCFT compression softening model with the possibility of refinement. As well, it allows for a critical examination of the various alternate models proposed, and of the significance of the factors thought to influence the softening.

Hence, this paper will address a number of objectives. A review will be made of some of the compression softening models proposed. Test programs completed subsequent to the formulation of the MCFT model, adding to the database, will also be reviewed. From the expanded data, a refined compression softening model will be sought, and the influence of various models available will be made.

MODELS FOR COMPRESSION SOFTENING

The original analytical model derived from test data proposed the use of a softening parameter β, with β being a function of the ratio of principal

tensile strain to principal compressive strain ($\varepsilon_1/\varepsilon_2$) (Vecchio and Collins 1982). It was argued that the deterioration in compression resistance exhibited by the concrete, due to cracking, was measurable by the eccentricity of the strain circle reflected in the ratio $\varepsilon_1/\varepsilon_2$. The compression softening observed was manifested in both the strength and ductility of the concrete. Thus, the proposed model involved modifying the Hognestad parabola, which was used as the base curve describing the uniaxial compressive response of concrete. Modifications were made to both the peak stress and the strain at peak stress, giving the softened curve shown in Fig. 2(*a*). The softening parameter β proposed was

$$\beta = \frac{1}{0.85 - 0.27\dfrac{\varepsilon_1}{\varepsilon_2}} \quad \ldots\ldots (1)$$

Good correlation with the test data was found. For the 178 data points collected in which f_{c2} exceeded $0.15 f_c'$, the ratio of experimental to predicted stress had a mean value of 1.01 and a coefficient of variation of 15.4%.

To facilitate the use of a softening model in design procedures for beams in shear, a simplified model was subsequently formulated (Vecchio and Collins 1986). The softening coefficient was made solely a function of the principal tensile strain ε_1. Again, the Hognestad parabola was used as the base curve, but the strain at which peak stress was attained was not reduced. The simplified model, shown in Fig. 2(*b*), used the following relationship for β:

$$\beta = \frac{1}{0.80 + 0.34\dfrac{\varepsilon_1}{\varepsilon_0}} \quad \ldots\ldots (2)$$

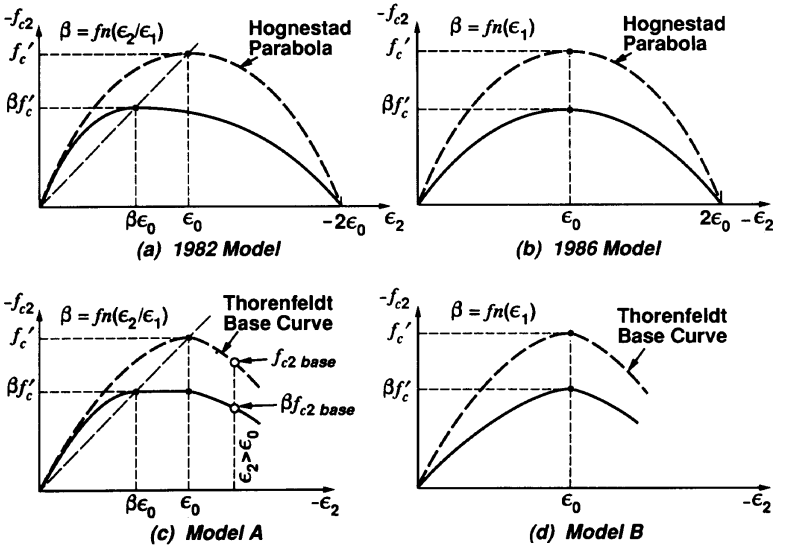

FIG. 2. Compression Softening Models: (*a*) 1982 Model; (*b*) 1986 Model; (c) Proposed Model A; (*d*) Proposed Model B

The correlation with the test data was almost as good, with the ratio of experimental to theoretical stress having a mean of 0.98 and a coefficient of variation of 16.4%.

A number of parallel investigations into compression softening of concrete have since been conducted elsewhere. There is considerable variation in the degree of softening observed, and in what are thought to be the key influencing variables.

Kollegger and Mehlhorn (1990) tested 47 panels (1,000 × 500 × 100 mm) at the University of Kassel, and eight panels at the University of Toronto. The Kassel specimens involved tension-compression loads applied parallel to the reinforcement directions, whereas some of their Toronto panels had principal stresses inclined at 45° to the reinforcement. Kollegger and Mehlhorn concluded that the effective compressive strength did not reduce beyond $0.80\,f'_c$, and that the prime influencing factor appeared to be the principal tensile stress f_{c1} rather than the principal tensile strain ε_1. It should be noted that none of the specimens tested were reinforced or loaded such that large tensile strains (and hence significant softening) could be achieved before behavior became governed by yielding of all reinforcement crossing the crack direction.

Miyahara et al. (1988) proposed a softening model as a function of the principal tensile strain. The relation suggested for the reduction in strength was

$$\beta = 1.0; \qquad \varepsilon_1 < 1.2 \times 10^{-3} \qquad \ldots\ldots (3)$$

$$\beta = 1.15 - 125\varepsilon_1; \qquad 1.2 \times 10^{-3} < \varepsilon_1 < 4.4 \times 10^{-3} \qquad \ldots\ldots (4)$$

$$\beta = 0.60; \qquad \varepsilon_1 > 4.4 \times 10^{-3} \qquad \ldots\ldots (5)$$

Again, the degree of softening represented in this relation was significantly less than that predicted by the Vecchio-Collins model. It should be noted, however, that this model is used together with a shear transfer model. In cases where appreciable levels of shear transfer act on the crack plane, the reduction effect is greater than that predicted by the compression model alone. In such cases, a direct comparison to the Vecchio-Collins model is difficult.

Shirai and Noguchi (1989) tested a number of uniaxially reinforced panels under tension-compressive states with loading applied in the reinforcement directions. They found that the concrete compressive strength and stiffness were significantly influenced by the average tensile strains, by the tensile force applied to the reinforcement, and by the bond properties of the reinforcing bars. Additional tests were later conducted in which the principal stress directions were skew to the reinforcement. Mikame et al. (1991) then noted differences in the degree of softening achieved in shear tests as compared to tension-compression tests. In their proposed model, the basic reduction factor, applied to the strength only, was suggested as

$$\beta = \frac{1}{0.27 + 0.96\left(\dfrac{\varepsilon_1}{\varepsilon_0}\right)^{0.167}} \qquad \ldots\ldots (6)$$

The base factor was then modified to allow for the influences of the angle between the reinforcement and the crack direction, the crack spacing, and the stress in the rebar. They also noted that the reduction was dependent

on the cylinder strength of the concrete (f'_c), and was greater in high-strength concrete. For high-strength concrete, Ueda et al. (1991) proposed use of the following:

$$\beta = \frac{1}{0.8 + 0.6(1{,}000\varepsilon_1 + 0.2)^{0.39}} \quad \ldots\ldots (7)$$

Belarbi and Hsu (1991) reported the results of 34 panels (1,400 × 1,400 × 180 mm) tested under various conditions of in-plane stress. Their data led them to differentiate between a softening coefficient for strains, β_ε, and one for stresses, β_σ. The suggested model, using the Hognestad parabola as a base [see Fig. 2 (*a*)], was:

$$\beta_\sigma = \frac{0.9}{\sqrt{1 + K_\sigma \varepsilon_1}} \quad \ldots\ldots (8)$$

$$\beta_\varepsilon = \frac{1}{\sqrt{1 + K_\varepsilon \varepsilon_1}} \quad \ldots\ldots (9)$$

where K_σ and K_ε depended on the orientation of the cracks to the reinforcement (θ), and on the type of loading as follows:

- Proportional loading

  $K_\sigma = 400; \quad \theta = 45°, 90° \quad \ldots\ldots (10)$

  $K_\varepsilon = 550; \quad \theta = 90° \quad \ldots\ldots (11)$

  $K_\varepsilon = 160; \quad \theta = 45° \quad \ldots\ldots (12)$

- Sequential loading

  $K_\sigma = 250; \quad \theta = 90° \quad \ldots\ldots (13)$

  $K_\sigma = 400; \quad \theta = 45° \quad \ldots\ldots (14)$

  $K_\varepsilon = 0; \quad \theta = 90° \quad \ldots\ldots (15)$

  $K_\varepsilon = 160; \quad \theta = 45° \quad \ldots\ldots (16)$

TORONTO TEST PROGRAMS

In the experimental work conducted at the University of Toronto, the approach adopted was to subject simple reinforced-concrete panel elements to uniformly applied, well-controlled edge loads representing general conditions of in-plane stress. Accordingly, two unique test facilities were constructed. The panel element tester devised was capable of loading 890 × 890 × 70 mm test specimens under any combination of in-plane stress. The design of the facility was such as to permit proportional or nonproportional loads that could be arbitrarily changed during the course of a test. The shell element tester, developed later, was capable of loading shell elements up to 1,450 × 1,450 × 350 mm in size under conditions of in-plane stress, bending, and out-of-plane shear. A number of test programs have been conducted using these facilities, with a total of 119 panel elements and 30 shell elements having been tested to date. Only those tests that involved homogeneously constructed panels subjected to uniform in-plane stresses will be included here.

The original test program involved the 30 panel elements (PV-series specimens) reported by Vecchio and Collins (1982). These panels were generally orthotropically reinforced and subjected to monotonically increasing loads. The majority of the tests involved pure shear loads, although some elements were subjected to uniaxial compression, combined biaxial compression and shear, reversed cyclic shear, and changing load ratios. The variables also included percentage of transverse reinforcement, percentage of longitudinal reinforcement, and concrete strength. Many of the panels were observed to fail by a brittle crushing or ductile shear-crushing failure of the concrete at stresses well below the cylinder crushing stress.

Bhide and Collins (1989) conducted an investigation involving 31 test panels, reinforced in one direction only and loaded in various combinations of tension and shear (PB-series specimens). Unexpected reserves of strength and ductility, well beyond first cracking, were observed in these panels. The effects of tension stiffening, aggregate interlock, and dowel action were judged to be significant in such elements.

A series of 10 panel elements (PC-series specimens), some with center perforations, were tested to study behavior and modeling accuracy in structures containing highly disturbed stress regions (Vecchio and Chan 1990). Loading conditions included pure shear, shear and biaxial compression, and shear and biaxial tension. Four of the panels tested were homogeneously reinforced and without perforations; these are included here.

To primarily study the effects of lateral compression on the pre- and postcracking tension response of reinforced concrete, a series of six panel elements were tested (PRC-series specimens). The orthogonally reinforced panels were subjected to conditions of tension-compression applied parallel to the reinforcement. Various nonproportional loading sequences were used.

To investigate possible scale effects, two parallel series of panels were tested by the University of Toronto and the Kajima Corporation of Japan. The Kajima panels were approximately 2.5 times larger than the Toronto panels but otherwise identical in terms of concrete strengths, reinforcement percentages and strengths, and loading conditions. Included here will be the six Toronto panels (TP-series specimens).

Kollegger and Mehlhorn (1990) tested eight specimens using the University of Toronto panel element tester (PK-series specimens). These orthotropically reinforced panels were subjected to various loading regimes including shear and proportional biaxial compression, shear and nonproportional biaxial compression, and tension-compression parallel to the reinforcement.

To study compression softening effects in high-strength concrete, a series of 12 panel specimens were tested (PA- and PHS-series specimens). Typically, these panels were lightly reinforced in one of the two reinforcement directions, and were subjected to various combinations of shear and proportional biaxial stress.

A number of shell elements were tested in the pilot program for the shell element tester facility. Three of the specimens tested (SE1, SE5, and SE6) were limited to in-plane loads only. Subsequently, four shell elements were tested which were constructed from high-strength concrete (specimens SE11–SE14). In all cases, the loading condition imposed was pure shear. Stevens et al. (1991) tested three shell element under reversed cyclic loads (specimens SE8–SE10). Finally, the behavior of prestressed elements was investigated through three partially prestressed shell elements (specimens PP1–PP3) (Marti and Meyboom 1992).

From the 116 test specimens considered, readings from 1,084 load stages were collected. Note that the readings at each load stage represent the average of 12–24 separate measurements. Specimen details and test results can be found in the references cited.

ANALYSIS OF TEST DATA

In examining the test data, it is important to be clear about the manner in which the principal compressive stresses in the concrete are calculated. Average stresses in the reinforcement are determined from average strains using basic elastic-plastic relationships. Thus

$$f_{sx} = E_s \cdot \varepsilon_x \leq f_{yx} \quad \ldots\ldots (17)$$

and

$$f_{sy} = E_s \cdot \varepsilon_y \leq f_{yy} \quad \ldots\ldots (18)$$

Applying conditions of equilibrium in the reinforcement directions gives the concrete stresses

$$f_{cx} = \sigma_x - \rho_x \cdot f_{sx} \quad \ldots\ldots (19)$$

$$f_{cy} = \sigma_y - \rho_y \cdot f_{sy} \quad \ldots\ldots (20)$$

and

$$v_{cxy} = \tau_{xy} \quad \ldots\ldots (21)$$

where σ_x, σ_y, and τ_{xy} = the uniform stresses applied to the element. The average principal compressive stress in the concrete is then calculated as

$$f_{c2} = \frac{f_{cx} + f_{cy}}{2} - \left[\left(\frac{f_{cx} - f_{cy}}{2}\right)^2 + (v_{cxy})^2\right]^{1/2} \quad \ldots\ldots (22)$$

In some of the softening models that have been developed, the stress-strain relationships used for the reinforcement included reduced stiffness and yield strengths to reflect the influence of the surrounding concrete. Reduced average reinforcement stresses result in lower calculated concrete stresses, f_{cx} and f_{cy}, and ultimately a lower principal compressive stress f_{c2}. Thus, the softening effect on the concrete would be perceived to be greater. This, in part, explains some of the variations in the degree of softening predicted by the various models.

In analyzing the test data collected, a number of screens were applied. They were as follows:

1. Only elements subjected to monotonic loads were considered; element subjected to cyclic loads were omitted.
2. Elements that were improperly cast or tested were omitted; but data from elements failing prematurely due to mechanical problems were considered up until the point of failure.
3. Load stages representing postultimate response were omitted.
4. Load stages at which the principal compressive strain was less than $0.10\varepsilon_0$ were omitted.

The principal compressive stresses were found to be significantly lower than one would calculate using a base (unsoftened) uniaxial model such as

the Hognestad parabola [see Fig. 3(*a*) and Fig. 4(*a*)]. When all load stages were considered, the ratio of the experimental to theoretical stress had a mean of 0.792 and a coefficient of variation of 30.0%. Considering only the ultimate load stages for the 45 elements failing by concrete crushing/shear, the ratio $f_{c2\text{-experiment}}/f_{c2\text{-base}}$ further deteriorated to a mean value of 0.629 and a coefficient of variation of 34.8%. Thus the compression softening effect seen was significant.

Several possibilities were considered for the prime variable influencing the softening effect. This was done with models using both a strength and strain softened response [as in Fig. 2(*a*)], and with models using a strength only softened response [as in Fig. 2(*b*)]. The best correlation to the test data was achieved using $\varepsilon_1/\varepsilon_2$ as the prime variable in a strength and strain softening model [see Fig. 3(*b*)]. A strength-only softening model using ε_1 as the prime variable gave somewhat less satisfactory correlation [see Fig. 3(*c*)]. Interestingly, a $\varepsilon_1/\varepsilon_2$-function applied to a strength only softening model, and a ε_1-function applied to a strength and strain softening model, each gave much poorer results. Points in favor of the $\varepsilon_1/\varepsilon_2$ formulation included superior correlation at ultimate load stages, and a significantly better statistical goodness of fit (i.e., *R*-factor).

The softening models previously presented used the Hognestad parabola as the base curve. The Hognestad parabola does not provide a good representation of the response of high-strength concrete, which tends to be somewhat more linear in its preultimate response. As well, in low-strength concretes ($f'_c < 20$ MPa), the Hognestad parabola tends to underestimate stresses at intermediate levels. Thus, various alternatives were considered, and it was found that the Thorenfeldt et al. (1987) model resulted in the best correlations for the full range of concrete strengths represented in the database. The Thorenfeldt base curve, later calibrated by Collins and Porasz (1989), is the following:

$$f_{c2\text{base}} = -f_p \cdot \frac{n \cdot \left(\frac{-\varepsilon_2}{\varepsilon_p}\right)}{(n-1) + \left(\frac{-\varepsilon_2}{\varepsilon_p}\right)^{nk}} \quad \ldots\ldots (23)$$

where

$$n = 0.80 + \frac{f_p(\text{MPa})}{17.} \quad \ldots\ldots (24)$$

$$k = 1.0; \qquad -\varepsilon_p < \varepsilon_2 < 0 \quad \ldots\ldots (25)$$

$$k = 0.67 + \frac{f_p(\text{MPa})}{62.}, \qquad \varepsilon_2 < -\varepsilon_p \quad \ldots\ldots (26)$$

The Thorenfeldt curve used in a strength and strain softening model is illustrated in Fig. 2(*c*); its use in a strength only softening model is shown in Fig. 2(*d*).

Kollegger and Mehlhorn (1990), and others, drew attention to the thought that the previous softening models tended to overestimate the softening effect in situations where behavior was governed by yielding of all reinforcement crossing the crack direction. To guard against this, it was found useful to define a limiting value of the principal tensile strain, ε_{1L}, to be

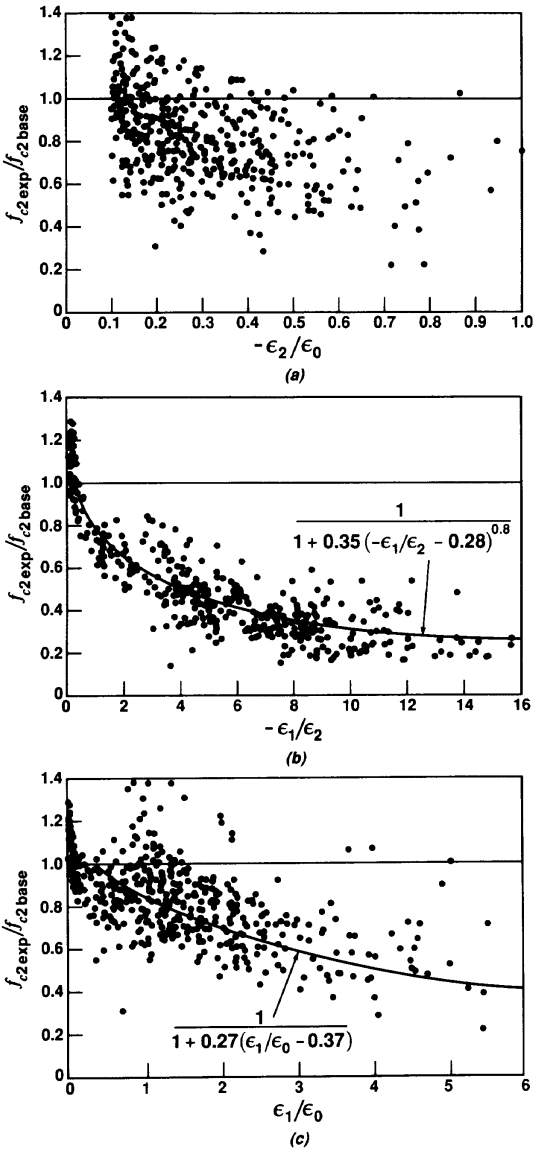

FIG. 3. Compressive Stress Data from Test Panels, Normalized by Stresses Calculated from Base (Unsoftened) Uniaxial Model Using Corresponding Measured Strains

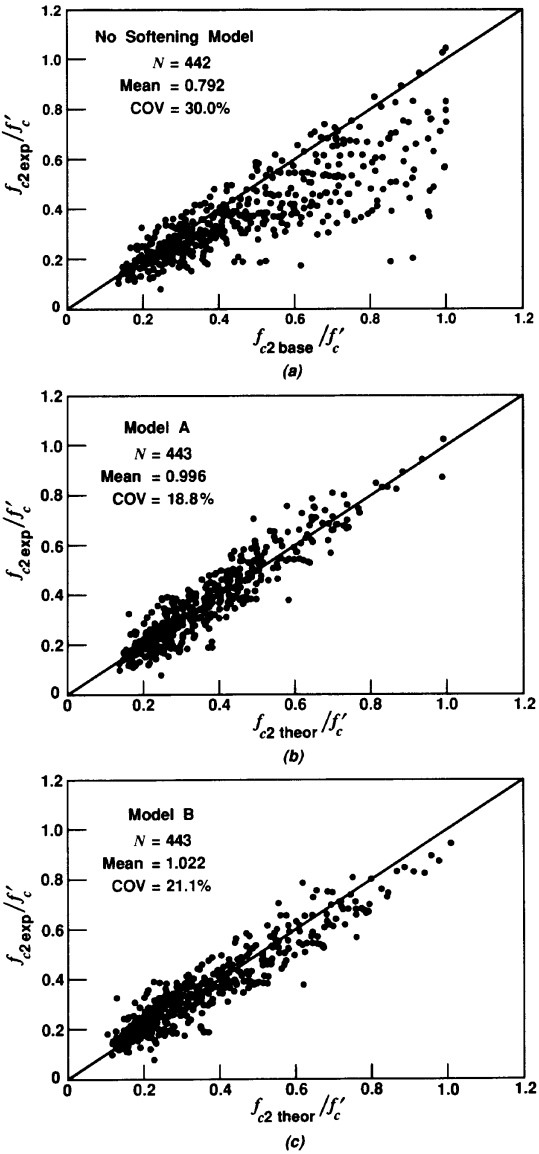

FIG. 4. Correlation of Test Panel Data: (*a*) Using No-Softening Model; (*b*) Using Softening Model A; (c) Using Softening Model B

used in the softening formulations. The criterion used to define ε_{1L} was the principal tensile strain at which the stresses in the reinforcement, at a crack, begin to limit the average principal tensile stress that can be developed in the concrete (i.e., f_{c1} limited by reinforcement yielding). At this strain level, little additional cracking can be inflicted on the concrete.

As Noguchi and others have observed, the softening effect may be more pronounced in high-strength concrete. This may be a consequence of smooth fracture planes forming, resulting in the earlier onset of local compression stability failure or in earlier crack-slip failure. This dependence on concrete strength was present in the data collected, but was not strong. Various formulations were considered by which the influence could be incorporated into the softening model. It was found that the most satisfactory results were obtained by imposing a multiplier, K_f, on the strain-related parameter $\varepsilon_1/\varepsilon_2$. The multiplier was found to be a function of the square root of the concrete strength.

Thus, based on statistical evaluations of the data, the strength and strain softening model shown in Fig. 2(*c*) was formulated. In what shall be referred to as model A, the softening factor β is given by

$$\beta = \frac{1}{1.0 + K_c K_f} \quad \ldots\ldots (27)$$

where

$$K_c = 0.35 \left(\frac{-\varepsilon_1}{\varepsilon_2} - 0.28 \right)^{0.80} \geq 1.0 \quad \ldots\ldots (28)$$

and

$$K_f = 0.1825\sqrt{f'_c} \geq 1.0 \quad \ldots\ldots (29)$$

Note that for $-\varepsilon_2$ less than $\beta \cdot \varepsilon_0$, f_{c2} is determined using (23) with $f_p = \beta \cdot f'_c$ and $\varepsilon_p = \beta \cdot \varepsilon_0$. For $-\varepsilon_2$ greater than ε_0, f_{c2} is equal to $\beta \cdot f_{c2\text{base}}$, where $f_{c2\text{base}}$ is found using $f_p = f'_c$ and $\varepsilon_p = \varepsilon_0$. In (28), ε_1 cannot exceed ε_{1L}.

For the 443 data sets considered, the ratio of the experimental to calculated stress obtained using the aforementioned model had a mean of 0.996 and a coefficient of variation of 18.8% [see Fig. 4(*b*)]. The goodness of fit (*R*-factor) was strong at 0.861. Considering the ultimate load stages of the 45 specimens failing by concrete crushing, the experimental to calculated stress has a mean of 1.06 and a coefficient of variation of 17.8%.

Only slightly weaker correlation was obtained by using a strength-only softening model as a function of ε_1. The optimal form attained, referred to as model B and illustrated in Fig. 2(*d*), was

$$\beta = \frac{1}{1 + K_c} \quad \ldots\ldots (30)$$

where

$$K_c = 0.27 \left(\frac{\varepsilon_1}{\varepsilon_0} - 0.37 \right) \quad \ldots\ldots (31)$$

Note that (23)–(26) are used with $f_p = \beta \cdot f'_c$ and $\varepsilon_p = \varepsilon_0$. No correlation could be found with f'_c and thus a K_f factor was not included. Using this model and considering all load stages, the ratio of experimental to calculated

principal compressive stress had a mean of 1.022 and a coefficient of variation of 21.1% [see Fig. 4(*c*)]. The correlation coefficient (*R*-factor) was significantly weaker at 0.682. Considering the ultimate stress conditions of the panels failing in concrete crushing, the stress ratio had a mean and coefficient of variation of 1.018% and 22.7%, respectively.

Parametric studies were undertaken to ascertain the influence of various factors on the degree of softening observed. In the comparisons that follow, the calculated stresses were determined using model A.

Consider first the dependence on the strength of the concrete. Shown in Tables 1 and 2 are the correlations between measured and calculated f_{c2}, with and without the K_f factor included, for various ranges of f'_c. When the concrete strength factor is not included, there is clearly more softening observed in the higher-strength concretes. Including the K_f factor brings about a more uniform degree of correlation for all ranges of f'_c.

Belarbi and Hsu (1991) have noted a dependence on the loading path,

TABLE 1. Influence of Primary Factors—Strain Ratio

		$f_{c2\text{-exp}}/f_{c2\text{-theor}}$			
		Without K_c		With K_c	
$-\varepsilon_1/\varepsilon_2$ (1)	N (2)	Mean (3)	COV (%) (4)	Mean (5)	COV (%) (6)
0–2	98	0.960	16.0	1.016	12.0
2–4	58	0.785	22.8	0.972	19.6
4–6	97	0.787	21.8	0.986	17.2
6–8	79	0.765	27.6	0.963	19.5
8–10	61	0.776	32.1	1.018	22.2
10–12	31	0.812	27.7	1.006	26.0
12–14	8	0.739	17.6	0.998	18.7
14–16	6	0.746	16.7	0.930	9.3
0–16	438	0.820	25.0	0.992	18.4

TABLE 2. Influence of Primary Factors—Concrete Strength

		$f_{c2\text{-exp}}/f_{c2\text{-theor}}$			
		Without K_f		With K_f	
f'_c (MPa) (1)	N (2)	Mean (3)	COV (%) (4)	Mean (5)	COV (%) (6)
10–20	87	1.046	11.8	1.046	11.8
20–30	230	1.007	20.3	1.007	20.3
30–40	10	1.082	16.0	1.096	15.2
40–50	34	0.844	13.8	0.894	16.4
50–60	53	0.884	12.4	0.975	15.8
60–70	13	0.873	12.3	0.961	13.5
70–80[a]	10	0.581	24.2	0.709	24.1
80–90[b]	6	0.758	23.4	0.905	35.8
10–90	443	0.972	19.9	0.996	18.8

[a]SE11/SE12
[b]SE13

TABLE 3. Influence of Secondary Factors

Variable (1)	$f_{c2\text{-exp}}/f_{c2\text{-theor}}$ N (2)	Mean (3)	COV (%) (4)
(*a*) Load Path			
Proportional	330	0.983	18.6
Nonproportional	113	1.031	19.5
Cyclic[a]	16	0.864	13.0
(*b*) Crack Orientation			
$0° \le \theta \le 15°$	106	1.040	17.9
$15° < \theta \le 30°$	22	0.898	21.2
$30° < \theta \le 45°$	315	0.987	18.8
(*c*) Crack Rotation			
$0° \le \Delta\theta \le 5°$	249	1.010	18.9
$5° < \Delta\theta \le 15°$	167	0.995	17.4
$15° < \Delta\theta \le 30°$	27	0.858	23.6
(*d*) Reinforcing Bar Type			
Mesh	139	0.976	15.3
Deformed bar	304	1.004	20.3
(*e*) Size			
Panel elements	372	1.008	17.6
Shell elements	52	0.921	24.7
Kajima specimens	19	0.944	24.7

[a]PV30 and final load stages of SE8, SE9, SE10.

and have produced different formulations for sequential (i.e., nonproportional) loading as opposed to proportional loading. Shown in Table 3 are the correlations obtained for three categories of loading among the tests considered here. There is essentially no difference in the accuracy of the model's predictions between the proportional and nonproportional loading cases. The limited data on the cyclic loading condition does, however, reflect some additional degradation in strength that is currently unaccounted for.

Noguchi suggested that the inclination of the stress field to the reinforcement influences the degree of softening. Specifically, greater softening is expected in cases where the crack direction is inclined to the reinforcement as compared to when the compression is orthogonal to the reinforcement grid. This may be the case in some models, depending on the manner in which f_{c2} is calculated (see earlier discussion). In Table 3, comparisons are made of the predictions of the model for various inclinations of the stress field. Again, there is little difference in the accuracy of the calculated values for the range of angles.

It has been suggested that the degree of crack rotation that occurs after first cracking may reflect in greater damage, and thus more softening. Shown in Table 3 are the correlations corresponding to various degrees of crack rotation (i.e., angle change in the principal strain direction). There appears to be some additional damage present in specimens where the change in crack direction exceeded 15°. However, the database for this condition was

not sufficient to formulate a relationship. No additional softening was observed in panels precracked in the perpendicular direction prior to loading.

While the majority of the test specimens were reinforced with deformed bars, some panels were reinforced with welded wire mesh. The wire mesh reinforced specimens typically tended to form a more closely spaced crack pattern. In Table 3, the observed to calculated stresses are compared for the two types of reinforcement. While the elements reinforced with wire mesh did exhibit slightly more softening, the differences were not significant.

Size effects and factors relating to the test facility used may also impact on the degree of softening perceived. Table 3 compares the correlations obtained from the panel elements (890 × 890 × 70 mm tested on the panel element tester) against those obtained for the shell elements (1,450 × 1,450 × 300 mm tested on the shell element tester). There is a definite difference between the two, with the shell-element specimens showing greater softening. It is not possible to determine whether this is a legitimate size effect, or whether it is related to the test facility or means of load application. Data from tests conducted elsewhere would be useful here.

COMPARISON OF MODELS

The various concrete compression softening models previously discussed were examined in their ability to model the behavior represented in the University of Toronto test data. The ratio of experimental to theoretical principal compressive stress was examined for each load-stage data point, subject to the same restrictions previously described. The results are summarized in Table 4.

Consider first the case where all load stages prior to and including ultimate load, for all specimens, are included. Model A gave the strongest correlation, with the ratio of experimental to theoretical compressive stress having a mean of 1.00 and a coefficient of variation of 18.8%. The Maekawa and the Noguchi models also gave good predictions of the mean stresses, but with somewhat higher scatter of results (coefficient of variation ≃ 23%). The Hsu model showed weaker correlation, overpredicting the softening effect and giving substantially higher scatter (coefficient of variation ≃ 26%). Limiting the softening effect to $0.80 f'_c$, as suggested by Mehlhorn, resulted in an underestimation of the compression softening effect and still higher scatter. Finally, not allowing for any compression softening, as seen in Table 4, led to unacceptably poor results. It is interesting to note that the original models, formulated 10 years ago before much of the test data was collected, continued to exhibit good correlation.

The observations noted here are reinforced when one examines the data at the condition of ultimate load for the 45 specimens that failed by concrete crushing (see Table 4). The Vecchio-Collins model continued to give calculated stresses that correlate well with the experimental values (mean 1.06; coefficient of variation 17.8%). The Maekawa and Noguchi models tended to underestimate the softening effect at ultimate load conditions, and with significant scatter in the results. The Hsu model gave a good mean prediction of stress, but again the scatter of results was significantly higher at 32%. Limiting the compression softening to $0.80 f'_c$ (i.e., Mehlhorn), or ignoring it altogether, resulted in severely overestimated strength at ultimate, with coefficients of variation in excess of 33%.

It is expected that the Vecchio-Collins formulation, derived from the database described herein, should best model this data. For this reason, a second database, derived from tests conducted elsewhere, was examined.

TABLE 4. Correlations with University of Toronto Data

Model (1)	$f_{c2\text{-exp}}/f_{c2\text{-theor}}$		
	N (2)	Mean (3)	COV (%) (4)
(*a*) All Load Stages			
Vecchio-Collins 1982	442	1.013	24.1
Vecchio-Collins 1986	442	0.993	26.8
Model A	443	0.996	18.8
Model B	443	1.022	21.1
Mehlhorn	442	0.905	26.1
Maekawa	442	0.996	24.4
Noguchi	442	0.973	23.2
Hsu	442	1.075	26.5
No softening	442	0.792	30.0
(*b*) Ultimate Load Stage in Concrete Crushing Specimens			
Vecchio-Collins 1982	45	1.103	23.4
Vecchio-Collins 1986	45	1.088	24.6
Model A	45	1.060	17.8
Model B	45	1.018	22.7
Mehlhorn	45	0.773	33.7
Maekawa	45	0.964	28.2
Noguchi	45	0.923	31.7
Hsu	45	1.036	31.8
No softening	45	0.629	34.8

Note: Models Vecchio-Collins (1982), Vecchio-Collins (1986) and Hsu et al. use Hognestad parabola as base curve; all others use Thorenfeldt base curve.

The data chosen were those reported by Belarbi and Hsu (1991), derived from tests performed on 22 panels. The panels were subjected to tension-compression stress conditions, with the loads applied parallel to the reinforcement directions. Several variations of sequential and proportional loading regimes were used.

Compared in Table 5 are the predictions of the Vecchio-Collins and Hsu models for conditions corresponding to the University of Houston test data. Consider first the results at the ultimate load stage of each of the test specimens. The Vecchio-Collins model slightly underestimated the observed softening effect with a mean of 0.92, while the Hsu model overestimated the softening with a mean of 1.18. Both models exhibited similar levels of scatter with coefficients of variation of about 15%. Consider next all load stages of the University of Houston test specimens for which $-\varepsilon_2$ exceeded 0.10 ε_0. As shown in Table 5, the Hsu model again overestimated the softening effect with a mean of 1.12. The scatter of the predictions, however, was extremely high with a coefficient of variation of 37.2%. The Vecchio-Collins model, on the other hand, continued to underestimate the softening observed in these tests, with a mean stress ratio of 0.86. However, the scatter of results was significantly better at 24.3%.

Belarbi and Hsu claimed that their model, in comparing the ratio of experimental to calculated peak stress softening coefficient, gave a mean of 1.02 and a coefficient of variation of 12.1%. This is somewhat misleading for the reason that the experimental and predicted peak compressive stresses

TABLE 5. Correlations with University of Houston Data

Model (1)	$f_{c2\text{-exp}}/f_{c2\text{-theor}}$		
	N (2)	Mean (3)	COV (%) (4)
(*a*) All Load Stages[a]			
Model A	250	0.861	24.2
Model B	250	0.869	28.1
Mehlhorn	250	0.751	26.5
Maekawa	250	0.906	28.0
Noguchi	250	0.841	26.8
Hsu	250	1.124	37.2
No softening	250	0.635	29.3
(*b*) Ultimate Load Stage			
Model A	20	0.921	15.3
Model B	20	0.880	19.9
Mehlhorn	20	0.789	12.5
Maekawa	20	0.861	13.0
Noguchi	20	0.821	15.0
Hsu	20	1.178	15.1
No softening	20	0.671	16.5

[a]Including postultimate.

were calculated at completely different compressive strains. For example, shown in Fig. 5 are the observed and calculated values for specimen E10-1A. At the ultimate load stage (LS13), the measured strain condition was $\varepsilon_1 = 25.930 \times 10^{-3}$ and $\varepsilon_2 = -0.928 \times 10^{-3}$, and the compressive stress in the concrete was -12.88 MPa ($0.349 f'_c$). Based on a strain of $\varepsilon_1 = 25.930 \times 10^{-3}$, for sequential loading, the Hsu model gives a peak stress factor of $0.329 f'_c$. Thus, their ratio of experimental to theoretical peak stress is claimed to be $0.349 f_c'/0.329 f'_c$, or 1.06. However at a compressive strain of $\varepsilon_2 = -0.928 \times 10^{-3}$, the Hsu constitutive relation for f_{c2} will give a calculated value of $0.223 f'_c$. Thus, in actual fact, the ratio of experimental to predicted stress is $0.349 f'_c/0.223 f'_c$ or 1.57, and not 1.06.

PREDICTING ELEMENT BEHAVIOR

To get an indication of the relative importance of the compression softening effect, and of the models used to represent it, a finite element study was undertaken. Each of the compression softening models previously described were implemented into a nonlinear finite element analysis program (TRIX). Program TRIX uses a total load, secant stiffness formulation; details of the formulation, and its application to the analysis of panels, are discussed elsewhere (Vecchio 1989). Analyses were conducted for each of the 14 panels in the PV-series of tests that ultimately failed by a shear-crushing failure of the concrete.

Compared in Table 6 are the panels' ultimate loads obtained from the analyses using each of the various softening models. It is seen that, under the conditions represented by these tests, the degree of softening captured in the model is quite important in being able to accurately predict load capacity. The two proposed models generally predicted the panels' responses

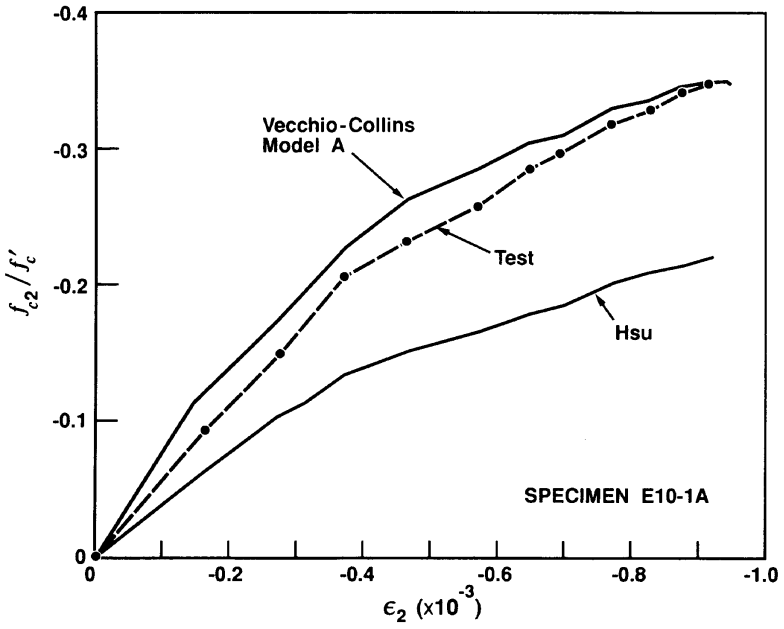

FIG. 5. Comparison of Experimental and Theoretical Compression Response of University of Houston Specimen E10-1A

accurately, giving a ratio of experimental to predicted strength of about 0.98, and coefficients of variation (COVs) of about 10%. The Hsu model tended to overestimate the softening effect, particularly in panels which did not experience yielding in either the transverse or longitudinal directions (i.e., panels PV22, PV23, PV25). The scatter of predictions was greatest with the Hsu model, with a COV of 14%. The proposed models and the Hsu model were able to accurately predict the failure mode, involving concrete crushing, in all cases.

The Maekawa and Noguchi models, each predicting relatively less compression softening of the concrete, tended to overestimate the strength of the panels. The ratios of observed to predicted strengths had means of 0.95 and 0.94, with COVs at 12% and 13%, respectively. It should be noted, however, that in many of the panels the predicted mode of failure changed from a concrete shear failure to one governed from yielding of the reinforcement in both directions.

The Mehlhorn model (allowing for little compression softening), and the null model (allowing for no compression softening), did not result in accurate predictions of behavior. For all panels, except PV17, PV23, and PV25, the predicted failure mode changed to one involving ductile yielding of the reinforcement. In some cases, this led to a significant overestimate of the strength and ductility of these panels.

Shown in Fig. 6 is the experimentally observed principal compression response of panel PV20. This panel failed by a shear-crushing failure of the concrete after yielding of the transverse reinforcement but prior to yielding of the longitudinal reinforcement. The concrete compression stress-strain response showed a considerable softening, attaining a peak value of 0.40

TABLE 6. Results of Finite Element Analysis

Specimen (1)	Experiment ultimate load (MPa) V_u (2)	$V_{u\,exp}/V_{u\,theor}$ Vecchio-Collins Model A (3)	Vecchio-Collins Model B (4)	Mehlhorn (5)	Maekawa (6)	Noguchi (7)	Hsu (8)	No softening (9)
PV10	3.97	1.056	1.056	1.056	1.056	1.056	1.056	1.056
PV12	3.13	1.054	1.091	1.023	1.047	1.036	1.057	1.013
PV17	−21.31[a]	1.022	1.022	1.022	1.022	1.022	1.022	1.022
PV18	3.03	0.974	0.974	0.910	0.921	0.921	0.932	0.902
PV19	3.95	0.988	0.980	0.921	0.936	0.932	0.952	0.931
PV20	4.26	0.945	0.934	0.897	0.899	0.899	0.920	0.897
PV21	5.03	0.892	0.900	0.879	0.878	0.879	0.942	0.878
PV22	6.07	0.909	0.906	0.835	0.902	0.837	1.071	0.835
PV23	8.88	1.153	1.118	0.976	1.220	1.118	1.375	0.835
PV25	9.13	1.100	1.057	1.033	1.072	1.130	1.312	0.885
PV26	5.41	0.867	0.870	0.867	0.868	0.870	0.925	0.867
PV27	6.24	0.898	0.897	0.791	0.888	0.825	1.045	0.790
PV28	5.61	0.908	0.920	0.860	0.860	0.858	1.051	0.858
PV29	5.87	0.920	0.730	0.736	0.791	0.709	0.892	0.550
Mean	—	0.978	0.961	0.915	0.954	0.935	1.039	0.879
COV (%)	—	8.9	10.7	10.6	11.9	13.0	13.8	13.9

[a] f_{x_u}

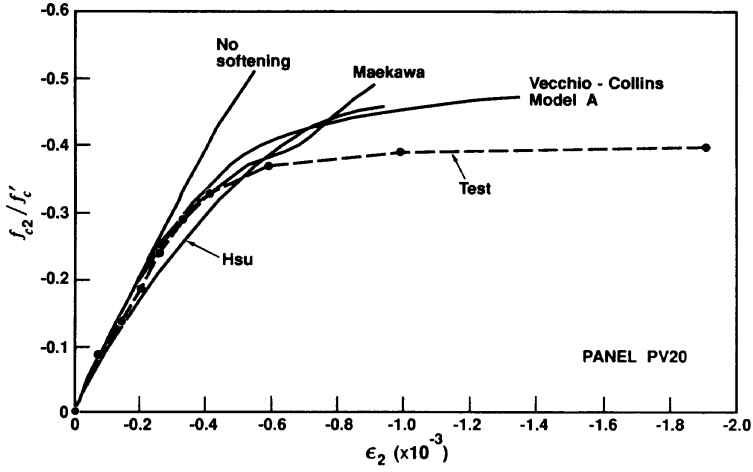

FIG. 6. Results of Finite Element Analyses of University of Toronto Panel PV20, Compared to Measured Response

f'_c with a significant accompanying reduction in stiffness. Shown also are the predicted responses, obtained from finite element analyses, using several of the compression softening models available. It should be noted at the outset that the predicted ultimate load, for this panel, was not influenced much by the compression model. If compression softening was ignored, the failure mode changed to one of yielding of both reinforcements at a load not much higher than the experimentally observed value. However, the predicted stiffness of the response was significantly greater than observed. The models that did allow for a substantial compression softening effect maintained the correct failure mode and better modeled the decay in the strength and stiffness of the concrete.

CONCLUSIONS

A number of analytical models have been proposed to represent the compression softening effect observed in cracked reinforced concrete in tension-compression states. In most of the models, the softening effect is tied to the degree of cracking that has occurred, measured by the average principal tensile strain. The various models available disagree significantly, however, as to the degree of softening that can occur.

In the past 10 years, a considerable volume of test data have been collected toward better quantifying the softening phenomenon. The data were generated from a wide range of specimen types, structural details, and loading conditions. Tests have been conducted at the University of Toronto, and elsewhere, using several different types of specially constructed testing rigs.

The data collected reveal that compression softening is clearly present and significantly influences the behavior of cracked reinforced concrete under certain conditions. It appears that the principal tensile strain is the single most important factor in dictating the degree of softening that was observed. Under monotonic loading conditions, the load path, crack orientation relative to the reinforcement, crack rotation, and reinforcing bar type appeared to have little or no influence on the degree of softening that

occurred. Concrete strength had some influence; slightly more softening was observed in high-strength concrete elements. As well, the data seems to suggest that there may be a size effect present.

Revised models were derived based on the new data available; however, they were not much changed from the original formulations developed 10 years ago. The revised models were found to give reasonably accurate predictions of the compression softening effect noted in the University of Toronto tests, and in specimens tested elsewhere.

A comparison of the various models available, together with the test data, showed considerable scatter in accuracy. The Hsu model overestimated the softening effect, coupled with high statistical scatter in the ratio of observed to predicted response. The Maekawa and Noguchi models tended to slightly underestimated the compression softening, and showed moderate levels of scatter. The Mehlhorn proposal, and discounting compression softening altogether, gave highly unconservative results, with large degrees of scatter. To be fair, however, some of the models (e.g., Maekawa, Noguchi) are coupled with shear transfer models, which make direct comparison difficult.

Analyses of overall element behavior, made using nonlinear finite element procedures, revealed that the accuracy of such analyses is generally better than that inherent in the compression softening models. The element behavior's dependence on the reinforcement, in many cases, tended to reduce the error in predicting response. Nevertheless, under certain conditions, neglecting or underestimating the compression softening effect resulted in significant overestimates of strength. As well, the failure mode and degree of ductility available, in these cases, were also grossly misjudged.

APPENDIX I. REFERENCES

Belarbi, A., and Hsu, T. T. C. (1991). "Constitutive laws of reinforced concrete in biaxial tension-compression." *Research Report UHCEE 91-2*, Univ. of Houston, Houston, Tex.

Bhide, S. B., and Collins, M. P. (1989). "Influence of axial tension on the shear capacity of reinforced concrete members." *ACT Struct. J.*, 86(5), 570–581.

Collins, M. P., and Mitchell, D. (1980). "Shear and torsion design of prestressed and non-prestressed concrete beams." *J. PCI.*, 25(5), 32–100.

Collins, M. P., and Porasz, A. (1989). "Shear strength for high strength concrete." *Bull. No. 193-Design Aspects of High Strength Concrete*, Comité Euro-International du Beton (CEB), 75–83.

Cook, W. D., and Mitchell, D. (1988). "Studies of disturbed regions near discontinuities in reinforced concrete members." *ACI Struct. J.*, 85(2), 206–216.

Kollegger, J., and Mehlhorn, G. (1990). "Experimentelle Untersuchungen zur Bestimmung der Druckfestigkeit des gerissenen Stahlbetons bei einer Querzugbeanspruchung." *Report 413*, Deutscher Ausschuss Für Stahlbeton, Berlin, Germany.

Marti, P., and Meyboom, J. (1992). "Response of prestressed elements to in-plane shear." *ACI Struct. J.*, 89(5), 503–514.

Mikame, A., Uchida, K., and Noguchi, H. (1991). "A study of compressive deterioration of cracked concrete." *Proc. Int. Workshop on Finite Element Analysis of Reinforced Concrete*, Columbia Univ., New York, N.Y.

Miyahara, T., Kawakami, T., and Maekawa, K. (1988). "Nonlinear behavior of cracked reinforced concrete plate element under uniaxial compression." Concrete Library International, *Japan Society of Civ. Engrs.*, JSCE, Vol. 11, 306–319.

Shirai, S., and Noguchi, H. (1989). "Compressive deterioration of cracked concrete." *Proc. ASCE Structures Congress 1989: Design, Analysis and Testing*, ASCE, New York, N.Y., 1–10.

Stevens, N. J., Uzumeri, S. M., Collins, M. P., and Will, G. T. (1991). "Constitutive model for reinforced concrete finite element analysis." *ACI Struct. J.*, 88(1), 49–59.

Thorenfeldt, E., Tomaszewicz, A., and Jensen, J. J. (1987). "Mechanical properties of high-strength concrete and application in design." *Proc. Symposium Utilization of High-Strength Concrete*." Stavanger, Norway, Tapir Trondheim.
Ueda, M., Noguchi, H., Shirai, N., and Morita, S. (1991). "Introduction to activity of new RC." *Proc. Int. Workshop on Finite Element Analysis of Reinforced Concrete*, Columbia Univ., New York, N.Y.
Vecchio, F. J. (1989). "Nonlinear finite element analysis of reinforced concrete membranes." *ACI Struct. J.*, 86(10), 26–35.
Vecchio, F. J., and Chan, C. C. L. (1990). "Reinforced concrete membrane elements with perforations." *J. Struct. Engrg.*, ASCE, 116(9), 2344–2360.
Vecchio, F. J., and Collins, M. P. (1986). "The modified compression field theory for reinforced concrete elements subjected to shear." *ACI J.*, 83(2), 219–231.
Vecchio, F. J., and Collins, M. P. (1982). "Response of reinforced concrete to in-plane shear and normal stresses." *Report No. 82-03*, Univ. of Toronto, Toronto, Canada.

APPENDIX II. NOTATION

The following symbols are used in this paper:

E_s = modulus of elasticity of reinforcement;
f'_c = nominal compressive strength of concrete (cylinder);
f'_t = nominal tensile strength of concrete;
f_{c1} = average principal tensile stress in concrete;
f_{c2} = average principal compressive stress in concrete;
f_{c2base} = compressive stress in concrete calculated from base curve;
f_{cx} = compressive stress in concrete in x-reinforcement direction;
f_{cy} = compressive stress in concrete in y-reinforcement direction;
f_p = maximum obtainable compressive stress in softened concrete;
f_{sx} = stress in x-direction reinforcement;
f_{sy} = stress in y-direction reinforcement;
f_{yx} = yield stress of x-direction reinforcement;
f_{yy} = yield stress of y-direction reinforcement;
K_c = coefficient reflecting influence of transverse tensile straining;
K_f = coefficient reflecting influence of nominal strength of concrete;
v_{cxy} = shear stress on concrete, relative to x-, y-axes;
β = concrete compression softening coefficient;
ε_1 = average principal tensile strain;
ε_{1L} = limiting principal tensile strain;
ε_2 = average principal compressive strain;
ε_o = strain in concrete cylinder at peak stress f'_c;
ε_p = strain in cracked concrete at peak stress f_p;
ε_x = strain in x-reinforcement direction;
ε_y = strain in y-reinforcement direction;
θ_{sc} = angle between reinforcement and normal to crack;
ρ_x = steel reinforcement ratio in x-direction;
ρ_y = steel reinforcement ratio in y-direction;
σ_x = normal stress applied to x-faces of element;
σ_y = normal stress applied to y-faces of element; and
τ_{xy} = shear stress applied to element faces.